Relaxation Dynamics of Piroxicam Structures within Human Serum Albumin Protein

Maged El-Kemary,[†] Michał Gil, and Abderrazzak Douhal*

Departamento de Química Física, ICAM, and Sección de Químicas, Facultad de Ciencias del Medio Ambiente, Universidad de Castilla-La Mancha, Avda. Carlos III, S.N., 45071, Toledo, Spain

Received December 11, 2006

We report on steady-state and ps-time-resolved emission studies of piroxicam (**1**) drug within human serum albumin (HSA) protein in cyclodextrin and in neat solvents. The steady-state results indicate that **1** binds to HSA protein and that two binding sites are involved. The fluorescence decays corresponding to site I in subdomain IIA and to site II in subdomain IIIA have time constants of ∼60 ps and ∼360 ps, respectively. The results suggest that the anion forms bind to site I, whereas the zwitterionic ones bind to site II. The energy-transfer process from excited tryptophan to **1** can occur with moderate efficiency (50%). The rotational time of **1** encapsulated by HSA indicates diffusion within the protein. These findings can be used for a better understanding of piroxicam and HSA interactions.

1. Introduction

Studying structural dynamics of drug−protein complexes is crucial for understanding the biological effects and functions of drugs in the body.[1] The nature of the interaction forces involved in drug−protein complexes plays a significant role in drug delivery and action.[2−6] Elucidating the nature of the interactions and the time scale involved provide insights into the mechanism of molecular recognition and the role of binding in protein dynamics and function.[7−10] Recently, femtosecond studies of dynamical solvation and local rigidity in a series of reversible conformations of human serum albumin (HSA[a]) have been reported at different pH values.[11] The results revealed that the changes in the solvation dynamics with pH are correlated with the conformational transitions and are related to their structure integrity.[11]

Piroxicam (**1**, Figure 1) is a nonsteroidal anti-inflammatory drug (NSAID). Depending on the pH of the medium, it can adopt different structures.[12] At neutral pH, under biologically relevant conditions, the anionic structure predominates (**1d**, Figure 1).[13] At the ground state it may exist in various conformations because of its ability to form inter- and intramolecular H-bonds. Upon electronic excitation of the closed enol structure (**1**) in nonpolar solvents, an intramolecular proton-transfer reaction takes place, transforming it to the keto-type form (**1b**, Figure 1).[14] The keto form has a ps-lifetime in the first electronically excited state (S_1) and a short-lived triplet state (7.5 ns).[15] In protic solvents, a second species called an open conformer (**1c**, Figure 1) is formed.[16] Furthermore, piroxicam caged within cyclodextrins (CD) and micelles was studied.[14,17,18] In CD, depending on the concentration of the guest relative to that of the host and on pH of the medium, it forms 1:1, 1:2, and 2:2 guest/host stoichiometry complexes.[14,17,19] At pH = 4, **1** in CD exists as the closed conformer **1b**.[14] In reverse micelles containing water, the anionic species predominates in addition to the presence of open and closed conformers.[18]

HSA protein is the most abundant one in blood plasma and it transports about 80% of a wide variety of fatty acids, metal ions, steroid hormones, vitamins, and drugs.[1−3] It also regulates the osmotic blood pressure.[1−3] The large plasticity of HSA is essential for the albumin molecule to accommodate a variety of ligands and to perform the transport function in the circulatory system.[11] When transporting a drug, the nature of the interactions involved in the stability of the drug−protein plays a significant role in drug delivery.[1−5] From the structural point of view, HSA is a single polypeptide chain consisting of 585 amino acids. Crystallographic studies indicate that at pH ≈ 7, it adopts a heart-shaped three-dimensional structure with three homologous domains I−III (Figure 1). Each domain contains two subdomains A and B.[6,20] The ligand binds to HSA in regions located in hydrophobic cavities in subdomains IIA (binding site I) and IIIA (binding site II). Binding to site I is dominated by the strong hydrophobic interactions with most neutral, bulky, heterocyclic compounds, while binding to site II mainly involves ion (dipole)−dipole, van der Waals, and/or H-bonding interactions in the polar cationic group of HSA.[6,21] Therefore, a detailed characterization of its effect on the structure and stability of a caged drug is essential for understanding the relevant keys for its physiological functions, delivery, and efficiency.

The interaction between piroxicam and HSA has been previously studied. It is spontaneous, exothermic, and involves H-bonds and hydrophobic forces.[22] It has been shown that **1** preferentially binds to site I (like warfarin) and has lesser affinity to site II (diazepam locus) of HSA.[23] The binding constants for each site were determined using equilibrium dialysis and are $K_1 = 2.3 \times 10^5\ M^{-1}$ and $K_2 = 3.3 \times 10^4\ M^{-1}$, respectively.[22] Although from the previous studies[22−24] it was not clear which structures of **1** binds to HSA sites and no photophysical study of the complexes has been yet published.

Here, we report on the excited-state dynamics of **1** in solution, in CD, and in HSA. The results provide information on the structural/conformational changes of **1** within HSA. We found that within the protein the anionic structure **1d** of piroxicam binds to site I and that possibly the zwitterionic form (**1e**, Figure 1) binds to site II of HSA. The anisotropy measurements show that the drug diffuses within the protein. Furthermore, upon excitation of HSA, energy transfer may occur from Trp214 of the protein to the caged **1**. Some neutral open structure **1c** binds to the surface of the protein and probably via H-bonding.

* To whom correspondence should be addressed. Tel.: +34-925-265717. Fax: +34-925-268840. E-mail: abderrazzak.douhal@uclm.es.

[†] Present address: Department of Chemistry, Faculty of Science, Kafr ElSheikh University, 33516 Kafr ElSheikh, Egypt.

[a] Abbreviations: NSAID, nonsteroidal anti-inflammatory drug; HSA, human serum albumin; CD, cyclodextrin; DM-β-CD, dimethyl-β-cyclodextrin; Trp214, tryptophan 214; EG, ethylene glycol; THF, tetrahydrofuran; CHX, cyclohexane; IRF, instrumental response function.

10.1021/jm061421f CCC: $37.00
Published on Web 05/17/2007

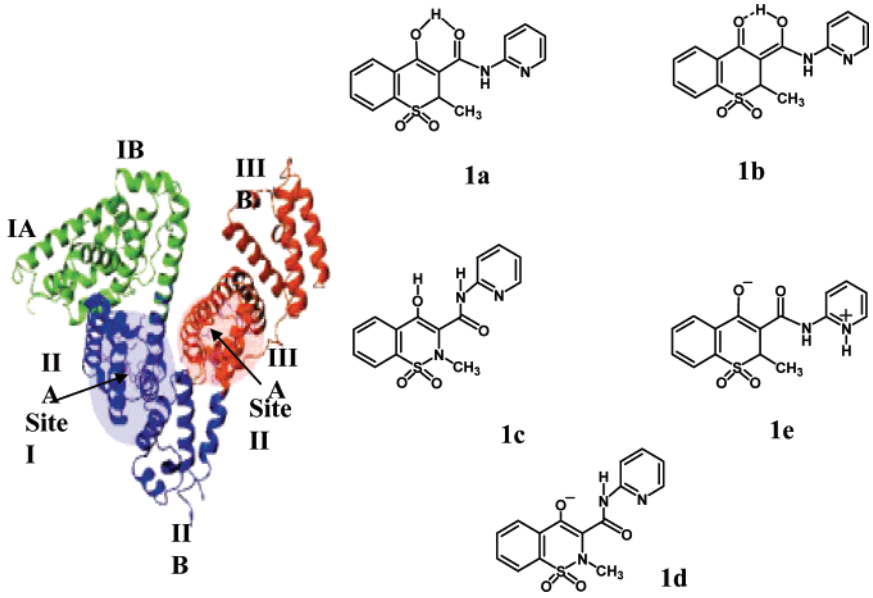

Figure 1. Crystalline structure of HSA (from ref 6) and possible structures of piroxicam (**1**): enol (**1a**), keto (**1b**), open (**1c**), anionic (**1d**), and zwitterionic (**1e**) forms.

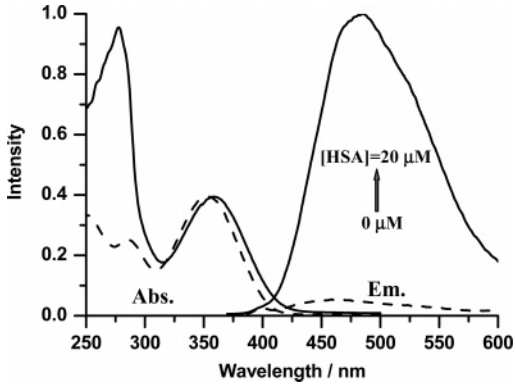

Figure 2. UV−visible absorption (left) and emission (right) spectra of **1** (2×10^{-5} M) in water buffer solution (pH 7.1) in the absence (− − −) and presence (—) of HSA (20 μM) and upon excitation at 355 nm.

2. Experimental Section

Piroxicam (1,2-benzothiazine-3-carboxamide-4-hydroxy-2-methyl-*N*-(2-pyridyl)-1,1-dioxide; 98%), HSA protein (99%, Sigma-Aldrich), and dimethyl-β-CD (DM-β-CD, 99%, Acros Organics) were used as received. All the solvents were spectroscopic grade (Sigma-Aldrich). We used a buffer of 50 mM sodium phosphate in Milli-Q water giving a pH ~7.1. Steady-state UV−visible absorption and emission spectra were recorded on Varian (Cary E1) and Perkin-Elmer (LS 50B) spectrophotometers, respectively. Emission decays were measured by a time-correlated single photon counting system described before.[25] The sample was excited by a 40 ps pulsed (20 MHz) laser centered at 371 nm, and the emission signal was collected at six wavelengths at magic angle. The instrumental response function (IRF) of the apparatus was typically 65 ps. Multiexponential functions convoluted with the IRF signal were fitted to the emission decays using the Fluofit package (PicoQuant). The quality of the fits was characterized in terms of residual distribution and reduced χ^2 value. All measurements were done at HSA concentration of 20 μM and at 293 ± 1 K.

3. Results and Discussion

3.1. Steady-State Observation. Figure 2 shows the UV−visible absorption and emission spectra of **1** in neutral water and in the presence of 20 μM of HSA. Upon addition of HSA, the absorption maximum at ~355 nm slightly shifts to 358 nm without change in the intensity, whereas the emission intensity is enhanced significantly with a shift from ~457 to 485 nm. These spectral changes indicate that **1** binds to HSA protein.

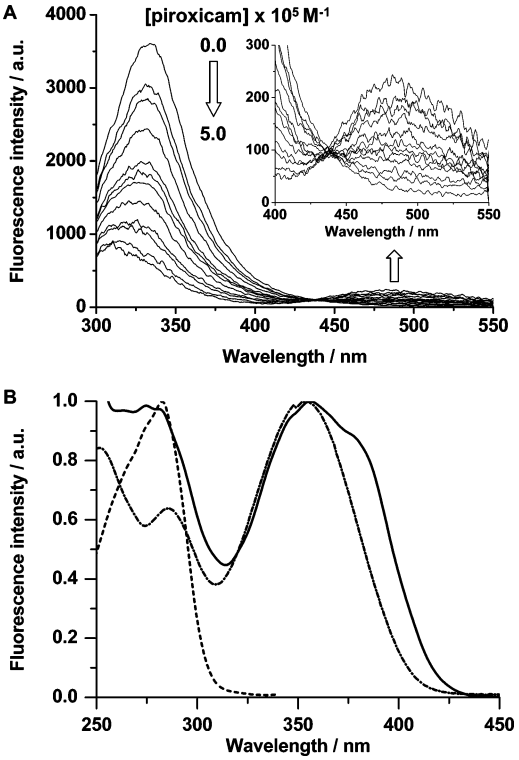

Figure 3. (A) Fluorescence spectra of HSA (20 μM) and piroxicam solutions in water at pH = 7.1 and at different drug concentrations (excitation at 280 nm). The emission intensity (I) of the spectra was corrected from reabsorption and inner filter effects, $I_{corr} = I_{obs} \times$ antilog $[(A(\lambda_{exc}) + (A(\lambda_{em}))/2]$, where A is the optical density at the excitation or emission wavelength. (B) Fluorescence excitation spectra of HSA (20 μM) in water (− − −) observed at 360 nm, piroxicam (20 μM) in water (− · −) observed at 480 nm and piroxicam in the presence of HSA (solid line) observed at 480 nm.

Figure 3A shows the change in the fluorescence spectra of the protein in the presence of different concentrations of **1** upon excitation at 280 nm. In neutral buffer solution, we observed a strong fluorescence band having a peak at 337 nm due to

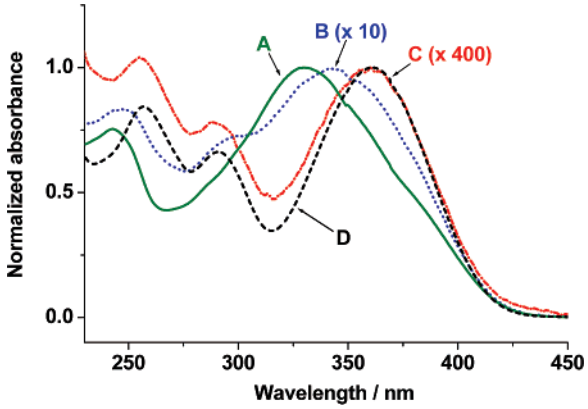

Figure 4. Normalized absorption spectra of **1** in EG at different concentrations: (A) 6×10^{-4} M (green); (B) 6×10^{-5} M (blue); (C) 1.5×10^{-6} M (red); (D) 6×10^{-4} M in alkaline EG (black).

tryptophan (Trp214) emission.[26] Addition of **1** causes a concentration-dependent quenching of Trp214 emission with a concomitant increase in the emission at ~490 nm, which is due to the bound **1**. The emission spectrum of HSA has the maximum at 337 nm and shifts to ~308 nm when increasing piroxicam concentration. This might be due (i) to a change in the local environment of Trp214 in HAS or (ii) that the remaining emission comes from the tyrosines of HSA. Another possible source of the blue shift that we cannot exclude is the increase of absorption of **1** when increasing its concentration. We believe that the decrease in Trp214 emission and the simultaneous increase in the piroxicam one suggest an energy-transfer process between HSA and the caged drug. The inset of Figure 3A shows an iso-emissive point at ~445 nm. Figure 3B shows that upon encapsulation of **1**, the $S_0 \rightarrow S_1$ transition of piroxicam shifts to longer wavelengths by 26 nm (1920 cm^{-1}). At pH 7.1 (and 9−12) the absorption at 355 nm is due to the anion of **1** (phenolate-type structure, **1d**).

Figure 3B shows the excitation spectra of free and HSA-caged **1** recorded at 480 nm. For the piroxicam spectrum, it is clear that the ratio between the intensity of the bands at ~360 and ~280 nm decreases (from 1.6 to 1) in presence of HSA. The change at 280 nm is due to Trp214 absorption when gating the emission of caged **1**. Therefore, an energy transfer process can occur upon excitation of Trp214 to produce an excited caged **1** emitting at 480 nm.

To understand the extent of the H-bonding interactions of **1**, with its restricting-motion environment, we have studied piroxicam in ethylene glycol (EG). The UV-absorption spectra at three different concentrations of **1** are shown in Figure 4. At a concentration of $\sim 10^{-5}$ M or larger, the absorption maximum of the first electronic transition shifts to shorter wavelengths and it stays at 330 nm when [piroxicam] $\geq 5 \times 10^{-5}$ M. For lower concentrations ($\leq 6 \times 10^{-6}$ M), the maximum appears at 361 nm. The presence of dimers/oligomers is unlikely in this range of concentrations and can be safely excluded. Another possible source of such a large blue shift is the ground-state hydrogen-bonding interaction of **1** with EG and formation of a conjugate anion of **1**, favored at low concentrations of the drug (Ostwald law for weak acid equilibrium). To support this explanation, we recorded the absorption spectrum of **1** in neutral and alkaline EG solutions (made by adding one KOH pellet to pure EG). After adding a small drop of alkaline EG to 6×10^{-6} M solution of **1**, we observed a spectral change similar to the effect of dilution (spectrum D in Figure 4). To further support this explanation, we added a small amount of water to a concentrated solution of **1** in EG and we observed no change

Table 1. Values of the Emission Lifetimes (τ_i) and Normalized Pre-Exponential Factors (a_i) from the Multiexponential Fit to the Fluorescence Decays of **1** in Different Media Observed at 460 nm[a]

medium	λ_A/nm	λ_F/nm	τ_1/ps	a_1%	τ_2/ps	a_2%	τ_3/ns	a_3%	χ^2
neutral buffer	355	455	<10	99.8			1.45	0.2	1.27
alkaline buffer[b]	355	464	<10	100					1.25
CHX	325	465	<10	5	58	95			1.25
THF	325	485	<10	5	49	95			1.27
EG[c]	361	480	35	96	100	4			1.23
EG[d]	330	480	35	32	100	68			1.04
HSA	358	490	61	47	359	32	1.47	21	1.14
DM-β-CD	356	436	30	95	180	4	2.20	1	1.07

[a] The table also contains the steady-state UV−visible absorption and fluorescence data of **1** in different media at maximum intensity. [b] pH ~ 9−12. [c] Value at concentration ~ 6×10^{-6} M. [d] Value at concentration ~ 6×10^{-4} M.

in relative contributions of the ps-emission components. The spectral position of the fluorescence band is not sensitive to the concentration change of the drug, and the maximum stays at 480 nm. Notice that the fluorescence quantum yield of the anionic form is very weak ($<10^{-5}$), so the CW-emission signal originates mainly from neutral keto-type **1b**. Time-resolved ps-measurements (vide infra) will give more information. In tetrahydrofuran (THF), the $S_0 \rightarrow S_1$ absorption maximum is located at 325 nm independently of piroxicam concentration (Table 1) and is due to enol **1** absorption. Upon excitation of this structure, a proton-transfer reaction takes place between the OH and C═O groups on the benzothiazine moiety, giving rise to emission of **1b**.

It is well-known that caging drugs by CDs can lead to a large change in their photochemical and photophysical events.[27] The hydrophobic interactions with the cage generally make the drugs to adopt other conformations generally not stable in water. The size of the cavity may restrict some photoprocesses of the drug as those of twisting or rotational motions. Therefore, we studied **1** in an aqueous solution of CD to compare its behavior with those observed in water and within HSA protein. Upon addition of DM-β-CD to a water solution at pH 7.1, we recorded a very small change in the absorption spectrum, suggesting a small variation in the molar absorption coefficient of the drug and/or weak complexation between **1** and CD. In contrast, in the presence of 20 mM of DM-β-CD, the emission intensity of **1** increases and shifts from 450 to 443 nm, indicating the formation of a complex. For the involved equilibrium, we found the binding constant $K = 62 \pm 10$ M^{-1}, assuming a 1:1 complex. This value is larger than that observed for β-CD at pH 4 (14.6 M^{-1})[14] and lower than that reported at pH 5.5 (134 M^{-1}).[17] The differences are explained in terms of CD ability to encapsulate and stabilize different structures of **1** in water at different pH.

3.2. Picosecond Emission Observation. 3.2.1. Water and Organic Media. To gain information on the dynamic relaxation of the excited state of the drug, we recorded ps-emission decays in different media. Figure 5 displays representative emission decays of **1** in a neutral buffer solution and in presence of DM-β-CD and HSA. Table 1 summarizes the obtained data from multiexponential fits of the decays. For THF (a polar solvent) and cyclohexane (CHX, a nonpolar solvent) solutions, we observed an ~50 ps decaying component (with a large contribution, 95%) and a faster decay (<10 ps, 5%), which could not be resolved by the used ps-apparatus. Our recent fs-experiments give a decaying (at the blue side) and a rising (at the red side) component of 2 ps. In aprotic solvents upon electronic excitation, piroxicam undergoes an intramolecular proton-transfer reaction.

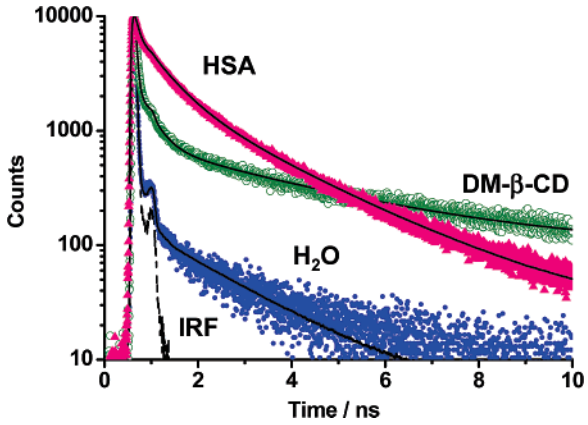

Figure 5. Emission decays of **1** in neutral water (blue), DM-β-CD (green), and HSA (red) solutions and gating at 460 nm. The data of the multiexponential fits (solid black lines) are shown in Table 1.

The short component might be due to **1b** undergoing a fast twisting motion of the bond connecting the main chromophor to the rest of the molecule. The longer component is suggested to be due to the emission of the neutral closed keto form, which probably comes from a twisted proton-transfer tautomer **1b** (Figure 1). This explanation is supported by the increase of the time constant value in a more viscous solvent (EG, 100 ps) and upon caging the drug by CD (180 ps). A previous study of **1** in CHX solution and under different experimental conditions of the excitation wavelength gives decay times of 58 ps (95%) and 180 ps (5%).[16] In the present study, we did not observe the 180 ps component.

In a more viscous solution like that of EG, the decays at the blue and red side of the emission band reveal the presence of two components with time constants of 35 ($\pm$10) ps and $\sim$100 ($\pm$20) ps. The contributions of these components do not show any observation-wavelength dependence. However, they change with the concentration of **1**, following the trend of the absorption spectrum mentioned in section 3.1. Decreasing the piroxicam concentration increases the relative population of anionic form **1d** (Figure 1). In fact, a decrease of the piroxicam concentration from 6×10^{-4} M to 6×10^{-6} M induces a decrease of the amplitude of the 100 ps component from 68% to $\sim$4%. The 100 ps component is then due to the keto tautomer **1b** formed after a fast ($<$10 ps) proton-transfer reaction in **1**. This lifetime is longer than the one found in THF due to the higher viscosity of EG. A decrease in its amplitude with the concentration of the **1** is accompanied by a relative increase of anionic form. The 35 ps component is than assigned to the anion, which finds hindrance to motion due to EG viscosity comparable to those of microemulsion and CD solutions. We measured also the lifetime of **1** in alkaline EG (prepared as said previously), and we found a monoexponential behavior giving $\tau = 50$ ($\pm$10) ps. This value is not very different from the one obtained for a diluted solution in neutral EG, taking into account quite different environment.

In a neutral water solution, the anionic form **1d** (Figure 1) predominates.[13] The fit of the decay recorded at 460 nm by a two-exponential function gives time constants of $<$10 ps ($\sim$99.8%) and 1.45 ns ($\sim$0.2%; Figure 5, Table 1). The contribution of these components does not show any significant change with emission wavelength. The shorter time ($<$10 ps) is assigned to the anionic form **1d** (Figure 1), as it is also reproduced by the fluorescence decay in alkaline buffer solutions (pH 9$-$12, Table 1). This value shows reasonable agreement with the previously reported lifetimes (16$-$20 ps and $\sim$98%) for anionic form of **1**.[14,18] Moreover, our recent fs-experiments at neutral and alkaline water solutions give an $\sim$4.5 ps decaying transient absorption band of the anion. The weak (0.2%) ns-component can be due to intermolecular H-bonding between **1c** and water molecules, as it has been previously assigned.[14,28] This assignment agrees with the reported solvatochromic analysis of **1**, which revealed that the H-bond donor ability of the solvent is the essential factor, which influences the spectral behavior of this molecule.[16,28]

3.2.2. CD and HSA Protein. In the presence of 20 mM of DM-β-CD (pH = 7.1), the fluorescence decay of **1** becomes longer, and three components were needed to get an accurate fit of the signal (Table 1). At 460 nm, we got 30 ps (with relative amplitude of 95%), 180 ps (4%), and 2.2 ns (1%). The shortest and the longest components correspond to those already found in the aqueous solution (Table 1). The intermediate component ($\tau_2 = 180 \pm 30$ ps), not observed in the absence of CD, is attributed to the caged drug, and it indicates the existence of the piroxicam/CD complex. The hydrophobic nature of the interior of the CD cage converts the anion **1d** to an enol caged **1a**, which is then phototransformed to the caged keto-type form **1b** having a lifetime of $\sim$180 ps. Using $K = 62$ M^{-1} as a value for an 1:1 complex formation and 20 mM of DM-β-CD, we estimate that $\sim$ 60% of **1** is not complexed. Therefore, the 30 ps component (of intensity contribution equal to 49%) is due to the free anion having a longer lifetime than in pure water ($<$10 ps), and the change is due to the expected increase in the viscosity of water upon addition of CD. This explanation is supported by a similar lifetime value of the anion in EG (35 ps). However, another source of this increase might come from the contribution of H-bonded structures (**1c**) of the drug attached to the external part of the cage, as it was observed in other systems.[29,30] In a previous study in acidic water (pH = 4), two different neutral species of **1** have been suggested to be encapsulated by β-CD, with the closed form of **1** and the open form **1c**.[14] We cannot make a direct comparison of the emission lifetime of **1** in the presence of CD at different pH values, as the involved complexes should be different. The emission lifetimes of these species are 60 and 130 ps, respectively.[14] However, in alkaline aqueous solutions of CD (pH = 10), no change in the fluorescence lifetime was observed, suggesting the absence of the inclusion process.[14]

To begin with the protein, when exciting it in water at 371 nm, the fit of the decay at 460 nm requires three exponential functions with time constants 166 ps (51%), 1.04 ns (32%), and $\sim$5 ns (17%). Previously, lifetime values of 680 ps (32%), 3.17 ns (38%), and 7.3 ns (30%) have been found when exciting at 295 nm.[31] The three exponentials decay arise from multiple protein conformations interacting differently with the environment.[31$-$33] For **1** in presence of 20 μM of HSA in neutral water, the decay fits give three components with time constants of 61 ps (47%), 359 ps (32%), and $\sim$1.47 ns (21%; Figure 5 and Table 1). Compared to water solution, in presence of HSA, a new component appears with a lifetime of 359 ps (32%). Furthermore, the amplitude of the ns-component significantly increases from 0.2 to 21%. In a parallel way, that of the shorter component decreases from 99.8 to 47%, and its lifetime ($<$10 ps) increases to 61 ps, indicating the formation of complexes with HSA. This behavior clearly reveals the presence of at least two emitters of **1** bound to HSA in addition to free **1** in solution. Using 20 μM of HSA and the reported binding constant values,[22] we estimated that 12% of **1** is free. The considerable difference between the steady-state emission maximum of piroxicam bound to HSA (490 nm) and that observed in DM-β-CD ($\approx$440 nm), suggests different emitting conformations of **1** in these cavities. Previ-

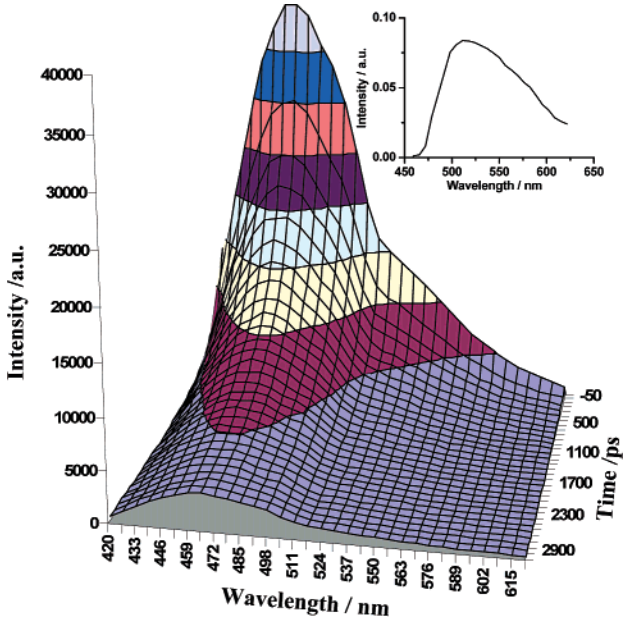

Figure 6. Time-resolved emission spectra of **1** in a neutral buffer solution (pH = 7.1) containing 20 μM of HSA. The excitation wavelength was 371 nm. The inset shows the difference between spectra gated at 100 ps and 1 ns.

ously, for β-CD, where the neutral form of **1** is included, a significant blue shift in the absorption maxima was observed from 360 to 330 nm.[14] In contrast, we found a slight variation in the absorption maximum of **1** (from 355 to 358 nm) when it binds to HSA. Therefore, it is possible that the anionic form **1d** is binding to HSA. The process might be assisted by the interaction of the anion with positively charged protein groups (e.g., $-NCH_3^+$). Such preferential binding of the anion compared to the neutral form has also been observed for ochratoxin and camptothecin.[34,35] We cannot also exclude the possibility of an excited-state intramolecular proton-transfer reaction leading to the keto form **1b** involving the protein moiety and acting as a proton-donor partner. The ns-component with a time constant of 1.47 ns (21%) might represent the contribution of the open neutral form **1c**, bound to the protein surface via intermolecular H-bonds. A study for protein surface and ligand interactions has been reported.[36] Note also that a contribution of the ~ns component might come from the intrinsic emission of HSA or its impurities (possibly oxidized aminoacids). Further more, due to the large flexibility of the protein, and a possible fast diffusion (see anisotropy part) of the drug, a ns-contribution due to a dynamical heterogeneity in the binding pocket cannot be excluded. As previously said, a report on the binding of **1** to HSA demonstrated that there are two locations of the drug within the protein with two different complexation constants: $K_1 = 2.3 \times 10^5\ M^{-1}$ and $K_2 = 3.3 \times 10^4\ M^{-1}$.[22] An equilibrium dialysis study reveals that **1** mainly binds to site I and, to a lesser extent, to site II.[23] Therefore, the higher binding constant ($2.3 \times 10^5\ M^{-1}$) is due to site I in subdomain IIA and the lower one ($K_2 = 3.3 \times 10^4\ M^{-1}$) is due to site II in the subdomain IIIA. Based on the above results, we propose that the ~60 ps lifetime with larger amplitude (47%) is due to the anion **1d** located at site I of the hydrophobic pocket IIA, while the ~360 ps (32%) is proposed due to zwitterionic structure **1e** in site II of the subdomain IIIA, and it mainly involves H-bonding and electrostatic interactions.[6,21,37,38] These structures emit at the red side of the spectrum, as it is shown by the time-resolved emission spectra (vide infra). A previous work on **1** in organic solvents suggested the coexistence of anion and zwitterionic

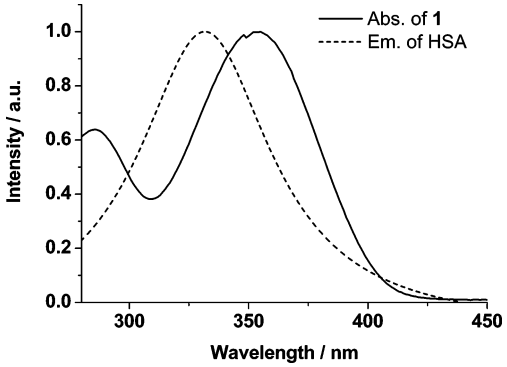

Figure 7. Spectral overlap between piroxicam absorption and HSA emission upon excitation at 280 nm in neutral buffer solutions ([HSA] = [piroxicam] = 20 μM).

forms.[39] According to the reported binding constants, the multiple binding of two molecules of piroxicam in two different sites of the same HSA takes place at a 1:1 molar ratio. Therefore, the influence of the piroxicam molecule bound in subdomain IIIA to the fluorescence decay of piroxicam bound in subdomain IIA of the same HSA molecule cannot be excluded.

Figure 6 shows picosecond time-resolved emission spectra (TRES) of **1** in a neutral aqueous solution containing 20 μM of HSA and upon excitation at 371 nm. It is clear that the nanosecond component in the emission decays appears at shorter wavelengths, whereas the picosecond one appears at longer wavelengths. This result clearly indicates the presence of different confined structures of **1** in the HSA having different environments leading to different degrees of robustness of the complex. The inset of Figure 6 shows the differences between the spectra gated at 100 ps and 1 ns. The difference gives the spectrum of the longtime-living component. In DM-β-CD at pH 7.1, we observed only a 1:1 inclusion complex with a relatively less degree of confinement.

3.3. Intermolecular Energy Transfer. The steady-state emission data obtained upon excitation of Trp214 (280 nm) and piroxicam (370 nm) suggest the existence of energy transfer from Trp214 to caged **1**. Figure 7 shows the overlap between the spectra of HSA emission and the spectra of piroxicam absorption. It indicates the possibility of energy transfer from the excited Trp214 residue to the bound **1**. As previously shown (Figure 3B), the excitation spectra of **1** in the presence of HSA suggest the energy transfer from Trp to caged piroxicam. The Förster theory for nonradiative energy transfer can be used to determine the distance between a donor (D) and an acceptor (A). The efficiency (E) of energy transfer from D to A is related to the distance (R) in this case between Trp214 and the drug according to eq 1[26]

$$E = 1 - \frac{\Phi}{\Phi_0} = \frac{R_0^6}{R_0^6 + R^6} \qquad (1)$$

where Φ_0 and Φ are the fluorescence quantum yield of the donor in the absence and presence of an equal amount of acceptor, respectively. R_0 is the Förster critical distance between A and D, at which 50% of the excitation energy is transferred to A and which can be obtained from D emission and A absorption spectra using eq 2[26]

$$R_0^6 = 8.8 \times 10^{-5} \kappa^2 n_D^{-4} \Phi_D \int_0^\infty I_D(\lambda) \epsilon_A(\lambda) \lambda^4 d\lambda \qquad (2)$$

$I_D(\lambda)$ is the normalized fluorescence spectrum of D and $\epsilon(\lambda)$ is the molar absorption coefficient of A. The fluorescence quantum

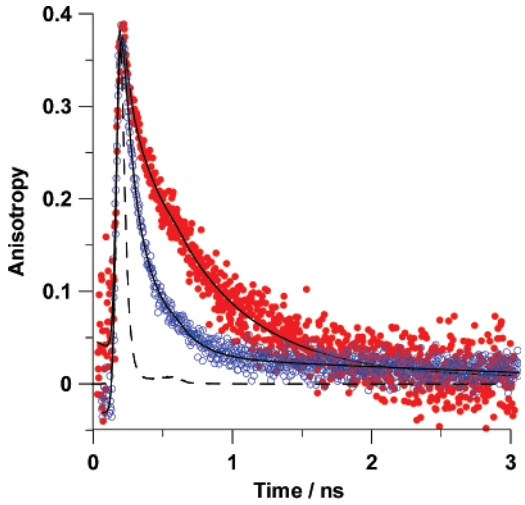

Figure 8. Anisotropy decay of **1** in the presence of 20 μM of HSA (blue) and 15 mM DM-β-CD (red) upon excitation at 371 nm and observation at 460 nm. The dashed line is IRF. The results of the multiexponential fits (solid lines) are shown in the text.

yield (Φ_D) of tryptophan in HSA is 0.11,[40] and the refractive index (n_D) of water is 1.333. The orientation factor (κ^2) is commonly taken as $^2/_3$, assuming a random orientation for both the donor and the acceptor.[41] This value is reasonable for the present system, as the tryptophan chromophore rotates very fast in the protein (isotropic system), as revealed by the ps-components in its emission anisotropy.[42−44] Using eq 2 yields R_0 = 23 Å. From eq 1, we obtained E = 0.5 and, thus, piroxicam−Trp214 distance (R) is 23 Å. Supposing that the energy transfer process is dominated by **1** bound in site I of subdomain IIA, the drug molecule is located ∼23 Å away from Trp214. Because we are considering the case of restricted mutual orientation of guest and host (orientation factor (κ^2) ≠ $^2/_3$), the obtained energy transfer distance should be considered as an upper limit value. Taking into account that the Trp214 rotates rapidly in the protein, the actual donor−acceptor distance can be estimated from a model of rotation in the cone semiangle of 30°.[34] This leads to the correction factor of 0.76−1.25,[34] giving in our case the actual value of R = 17.5−29 Å.

According to the Förster theory, the rate constant of energy transfer (k_{ET}) from Trp214 to **1** is given by eq 3

$$k_{ET} = \tau_{HSA}^{-1}(R_0/R)^6 \qquad (3)$$

where τ_{HSA} is the mean fluorescence lifetime of the tryptophan in HSA, τ_{HSA} = 3.53 ns.[31] Using this lifetime, efficiency of energy transfer 0.5, and eq 3, we got a lower limit of $k_{ET} = 2.8 \times 10^8$ s^{-1}. Förster energy transfer from excited donor to unexcited acceptor has rate constants in the range of 10^6−10^{11} s^{-1}.[40] The energy transfer between Trp214 and **1** obtained here has moderate value, but the process is still fast enough to compete with radiative deactivation of tryptophan. Previously, comparable values of k_{ET} and Trp214−guest distances have been reported.[31,34,40] As **1** binds much stronger to site I, we suggest that the energy transfer occurs from the excited Trp214 to piroxicam bound in subdomain IIA.

3.4. Time-Resolved Anisotropy. To gain further information on the binding interactions and rotational motions of the drug, we have performed time-resolved emission anisotropy measurements of **1** in neutral buffer, DM-β-CD, and in HSA solutions. Figure 8 shows representative anisotropy r(t) decays of **1** in HSA and in DM-β-CD at 460 nm. In neutral buffer solution (not shown), the decay fits to a single-exponential function with a rotational time of 20 ps. Using the Stokes−Einstein−Debye hydrodynamics theory[45,46] and modeling **1** as a prolate ellipsoid, we calculate the rotational relaxation times to be 90 and 27 ps under stick- and slip-boundary conditions, respectively. Our experimental value (20 ps) is close to that calculated under slip-conditions, suggesting that the emission depolarization is due to a fast conformational change, which should lead to a different electronic structure at S_1 strongly affecting the emission transition moment. This behavior agrees with the observed reaction in the excited **1** leading to an emission from the anion **1d** in water.

However, in DM-β-CD, we observed rotational times of ϕ_1 = 20 ps (66%), ϕ_2 = 210 ps (8%), and ϕ_3 = 600 ps (26%; χ^2 = 1.14). The shortest one is the same as the one found in water without CD and is assigned to the population of the uncomplexed drug. The longest one can be assigned to a rigid inclusion complex, as its value is similar to previously reported rotational times of DM-β-CD complexes.[7,8] We propose to assign the intermediate component to rotational time of the fraction of the drug, which is more loosely complexed to CD. We suggest two possibilities: (i) inclusion complexes where the drug can rotate within its cavity, suggesting a weak docking of the guest or inclusion through the phenyl part and (ii) H-bonded complexes of the drug to the exterior wall of CD, as it was observed in others systems.[29,30]

For HSA solution, the anisotropy decay of **1** shows a three-exponential behavior (Figure 8), giving rotational time constants ϕ_1 = 20 ps (70%), ϕ_2 = 170 ps (25%), and ϕ_3 = 20 ns (5%; χ^2 = 1.03). The first one is due to free **1** in solution. The ns-component is present in our time-window as a small and flat background. It was fixed with a value equal to the rotational time of typical robust dye/protein complexes[43] and, therefore, assigned to HSA tumbling motion. The 170 ps component we assigned to the rotational time of the drug population that can rotate within the protein cage. Rotational times in the ps−ns regime have been reported for aromatic guests in different proteins.[8,31,46] The observed rotational time value of included **1** (170 ps) is >100 times shorter than the global motion of HSA (∼20 ns),[43] indicating a diffusive motion of the drug in the hydrophobic pockets of the protein.

The value of the initial anisotropy (0.38) is close to the ideal one (0.40), and it suggests a small angle between the transition moments of absorption and emission.

4. Conclusion

This study provides clues for the binding properties and the dynamics of the interaction of piroxicam with HSA at neutral pH conditions. Time-resolved fluorescence measurements indicate the presence of different structures of piroxicam complexed to the HSA protein, having different locations and degrees of penetration/confinement. Anionic species are the most populated forms. The rotational time (∼170 ps) observed in the fluorescence anisotropy decay indicates that piroxicam diffuses within the protein. Moderately efficient energy transfer (50%) between excited Trp214 and bound piroxicam can occur. The Förster energy transfer rate constant is 2.8 × 10^8 s^{-1} and the estimated distance between Trp214 and the piroxicam is ∼23 Å.

Acknowledgment. This work was supported by the "Consejeria de Sanidad" and "Consejeria de Educacion y Ciencia" of JCCM and MEC through projects SAN-04-000-00, PBI-05-046, and CTQ2005-00114, respectively.

References

(1) Pethig, R. Protein-water interactions determined by dielectric methods. *Annu. Rev. Phys. Chem.* **1992**, *43*, 177−205.
(2) Peters, T., Jr. Ligand Binding by Albumin. All About Albumin. *Biochemistry Genetics and Medical Applications*; Academic Press: San Diego, 1996; pp 76−132.
(3) Carter, D. C.; Ho, J. X. Structure of serum albumin. *Adv. Protein Chem.* **1994**, *45*, 153−203.
(4) Settle, W.; Hegeman, S.; Featherstone, R. M. In *Handbook of Experimental Pharmacology*; Brodie, B., Gillette, J. R., Eds.; Springer-Verlag: Berlin, 1971; Vol. 28, pp 175−186.
(5) Kragh-Hansen, U. Molecular aspects of ligand binding to serum albumin. *Pharmacol. Rev.* **1981**, *33*, 17−53.
(6) He, X. M.; Carter, D. C. Atomic structure and chemistry of human serum albumin. *Nature* **1992**, *358*, 209−215.
(7) Zhong, D. P.; Douhal, A.; Zewail, A. H. Femtosecond studies of protein-ligand hydrophobic binding and dynamics: Human serum albumin. *Proc. Natl. Acad. Sci.* **2000**, *97*, 14056−14061.
(8) Douhal, A.; Sanz, M.; Tormo, L. Femtochemistry of orange II in solution and in chemical and biological nanocavities. *Proc. Natl. Acad. Sci.* **2005**, *102*, 18807−18812.
(9) Mataga, N.; Chosrowjan, H.; Taniguchi, S. J. Investigations into the dynamics and mechanisms of ultrafast photoinduced reactions taking place in photoresponsive protein nanospaces (PNS). *J. Photochem. Photobiol., C* **2004**, *5*, 155−168.
(10) Zhong, D.; Pal, S. K.; Wan, C.; Zewail, A. H. Femtosecond dynamics of a drug−protein complex: Daunomycin with apo riboflavin-binding protein. *Proc. Natl. Acad. Sci.* **2001**, *98*, 11873−11878.
(11) Qiu, W.; Zhang, L.; Okobiah, O.; Yang, Y.; Wang, L.; Zhong, D.; Zewail, A. H. Ultrafast solvation dynamics of human serum albumin: Correlations with conformational transitions and site-selected recognition. *J. Phys. Chem. B* **2006**, *110*, 10540−10549.
(12) Tsai, R.-S.; Carrupt, P.-A.; El-Tayar, N.; Giroud, Y.; Andrade, P.; Testa, B.; Bree, F.; Tillement, J.-P. Physicochemical and structural properties of non-steroidal anti-inflammatory oxicams. *Helv. Chim. Acta* **1993**, *76*, 842−854.
(13) Andrade, S. M.; Costa, S. M. B. Fluorescence studies of the drug Piroxicam in reverse micelles of AOT and microemulsions of Triton X-100. *Prog. Colloid Polym. Sci*. **1996**, *100*, 195−200.
(14) Kim, Y. H.; Cho, D. W.; Kang, S. G.; Yoon, M.; Kim, D. Excited-state intramolecular proton transfer emission of piroxicam in aqueous β-cyclodextrin solutions. *J. Lumin*. **1994**, *59*, 209−217.
(15) Cho, D. W.; Kim, Y. H.; Yoon, M.; Jeoung, S. C.; Kim, D. Dynamics of excited-state intramolecular proton transfer reactions in piroxicam. Role of triplet states. *Chem. Phys. Lett.* **1994**, *226*, 275−280.
(16) Andrade, S. M.; Costa, S. M. B. Hydrogen bonding effects in the photophysics of a drug, piroxicam, in homogeneous media and dioxane-water mixtures. *Phys. Chem. Chem. Phys*. **1999**, *1*, 4213−4218.
(17) Banerjee, R.; Chakraborty, H.; Sarkar, M. Host−guest complexation of oxicam NSAIDs with β-cyclodextrin. *Biopolymers* **2004**, *75*, 355−365.
(18) Andrade, S. M.; Costa, S. M. B.; Pansu, R. The influence of water on the photophysical and photochemical properties of Piroxicam in AOT/iso-octane/water reversed micelles. *Photochem. Photobiol*. **2000**, *71*, 405−412.
(19) Rozou, S.; Voulgari, A.; Antoniadou-Vyza, E. The effect of pH dependent molecular conformation and dimerization phenomena of piroxicam on the drug:cyclodextrin complex stoichiometry and its chromatographic behaviour: A new specific HPLC method for piroxicam: cyclodextrin formulations. *Eur. J. Pharm. Sci.* **2004**, *21*, 661−669.
(20) Wardell, M.; Wang, Z.; Ho, J. X.; Robert, J.; Ruker, F.; Ruble, J.; Carter, D. C. The atomic structure of human methemalbumin at 1.9 A. *Biochem. Biophys. Res. Commun*. **2002**, *291*, 813−819.
(21) Rosenoer, V. M.; Oratz, M.; Rothschild, M. A. *Albumin Structure, Function, and Uses*; Pergamon: Oxford, 1977.
(22) Oyekan, A. O.; Thomas, W. O. A. The energetics of the interaction of piroxicam with plasma albumin. *J. Pharm. Pharmacol*. **1984**, *36*, 831−834.
(23) Bree, F.; Urien, S.; Nguyen, P.; Albengres E.; Tillement, J. P. A re-evaluation of the HSA-piroxicam interaction. *Eur. J. Drug Metab. Pharmacokinet.* **1990**, *15*, 303−307.
(24) Trnavská, Z.; Trnavský, K.; Žlnay, D. Binding of piroxicam to synovial fluid and plasma proteins in patients with rheumatoid arthritis. *Eur. J. Clin. Pharmacol*. **1984**, *26*, 457−461.
(25) Organero, J. A.; Tormo, L.; Douhal, A. Caging ultrafast proton transfer and twisting motion of 1-hyroxyl-2-acetonaphthone. *Chem. Phys. Lett*. **2002**, *363*, 409−414.
(26) Lakowicz, J. R. *Principles of Fluorescence Spectroscopy*, 2nd ed.; Kluwer Academic/Plenum Publishers: Boston, 1999.
(27) El-Kemary, M.; Douhal, A. Photochemistry and photophysics of cyclodextrin caged drugs. In *Cyclodextrin materials photochemistry, photophysics and photobiology*; Douhal, A., Ed.; Elsevier: New York, 2006; Chapter 4.
(28) Andrade, S. M.; Costa, S. M. B.; Pansu, R. Structural changes in W/O Triton X-100/cyclohexane-hexanol/water microemulsions probed by a fluorescent drug Piroxicam. *J. Colloid Interface Sci*. **2000**, *226*, 260−268.
(29) Hazra, P.; Chakrabarty, D.; Chakraborty, A.; Sarkar, N. Intramolecular charge transfer and solvation dynamics of Nile Red in the nanocavity of cyclodextrins. *Chem. Phys. Lett*. **2004**, 388, 150−157.
(30) Organero, J. A.; Tormo, L.; Sanz, M.; Roshal, A.; Douhal, A. Complexation effect of γ-cyclodextrin on a hydroxyflavone derivative: Formation of excluded and included anions. *J. Photochem. Photobiol., A* **2007**, *188*, 74−82.
(31) Kamal, J. K. M.; Behere, D. V. Spectroscopic studies on human serum albumin and methemalbumin: Optical, steady-state, and picosecond time-resolved fluorescence studies, and kinetics of substrate oxidation by methemalbumin. *J. Biol. Inorg. Chem*. **2002**, *7*, 273−283.
(32) Vos, K.; Van Hoek, A.; Visser, A. J. Application of a reference convolution method to tryptophan fluorescence in proteins. A refined description of rotational dynamics. *Eur. J. Biochem*. **1987**, *165*, 55−63.
(33) Davis, D. M.; Mcloskey, D.; Birch, D. J.; Gellert, P. R.; Kittlety, R. S.; Swart, R. M. The fluorescence and circular dichroism of proteins in reverse micelles: Application to the photophysics of human serum albumin and *N*-acetyl-L-tryptophanamide. *Biophys. Chem.* **1996**, *60*, 63−77.
(34) Il'ichev, Y. V.; Perry, J. L.; Simon, J. D. Interaction of ochratoxin a with human serum albumin. Preferential binding of the dianion and pH effects. *J. Phys. Chem. B* **2002**, *106*, 452−459.
(35) Burke, T. G.; Mi, Z. H. Preferential Binding of the Carboxylate Form of Camptothecin by Human Serum Albumin. *Anal. Biochem.* **1993**, *212*, 285−287.
(36) Das, K.; Smirnov, A. V.; Wen, J.; Miskovsky, P.; Petrich, J. W. Photophysics of hypericin and hypocrellin A in complex with subcellular components: Interactions with human serum albumin. *Photochem. Photobiol*. **1999**, *69*, 633−645.
(37) Yamasaki, K.; Miyoshi, T.; Maruyama, T.; Takadate, A.; Otagiri, M. Characterization of region Ic in site I on human serum albumin. Microenvironmental analysis using fluorescence spectroscopy. *Biol. Pharm. Bull*. **1994**, *17*, 1656−1662.
(38) Aki, H.; Yamamoto, M. Thermodynamic characterization of drug binding to human serum albumin by isothermal titration microcalorimetry. *J. Pharm. Sci.* **1994**, *83*, 1712−1716.
(39) Banerjee, R.; Sarkar, M. Spectroscopic studies of microenvironment dictated structural forms of piroxicam and meloxicam. *J. Lumin*. **2002**, *99*, 255−263.
(40) Sytnik, A.; Litvinyuk, I. Energy transfer to a proton-transfer fluorescence probe: Tryptophan to a flavonol in human serum albumin. *Proc. Natl. Acad. Sci. U.S.A.* **1996**, *93*, 12959−12963.
(41) Vazquez-Ibar, J. L.; Weinglass, A. B.; Kaback, H. R. Engineering a terbium-binding site into an integral membrane protein for luminescence energy transfer. *Proc. Natl. Acad. Sci. U.S.A.* **2002**, *99*, 3487−3492.
(42) Maliwal, B. P.; Lakowicz, J. R. Effect of ligand binding and conformational changes in proteins on oxygen quenching and fluorescence depolarization of tryptophan residues. *Biophys. Chem.* **1984**, *19*, 337−344.
(43) Marzola, P.; Gratton, E. Hydration and protein dynamics: Frequency domain fluorescence spectroscopy on proteins in reverse micelles. *J. Phys. Chem*. **1991**, *95*, 9488−9495.
(44) Hansen, J. E.; Rosenthal, S. I.; Fleming, G. R. Subpicosecond fluorescence depolarization studies of tryptophan and tryptophanyl residues of proteins. *J. Phys. Chem*. **1992**, *96*, 3034−3040.
(45) Hu, C.; Zwanzig, R. Rotational friction coefficients for spheroids with the slipping boundary condition. *J. Chem. Phys.* **1974**, *60*, 4354−4357.
(46) Baskin, J. S.; Zewail, A. H. Molecular structure and orientation: Concepts from femtosecond dynamics. *J. Phys. Chem. A* **2001**, *105*, 3680−3692.

JM061421F